From end-of-life tires to storable energy carriers

Amandine Niezgoda, Yimin Deng, Florian Sabatier, Renaud Ansart

From end-of-life tires to storable energy carriers

A. Niezgoda [a], Y. Deng [b], F. Sabatier [c], R. Ansart [c,*]

[a] Toulouse INP-ENSIACET, Toulouse, France
[b] Beijing University of Chemical Technology, Beijing Advanced Innovation Centre for Smart Matter Science and Engineering, Beijing, China
[c] Laboratoire de Génie Chimique, Université de Toulouse, CNRS, INPT UPS, Toulouse, France

A B S T R A C T

End-of-life tires are an increasingly important environmental burden. Since retreading is only partly possible, safe and economic methods of disposal need to be developed. Pyrolysis of ELTs, and subsequent upgrading/application of the produced energy carriers, is considered a valuable treatment method. In order to design the process, numerous operation units have to be taken into account. Char, vapour and gas are formed in the reactor. The char is purified from ZnO with a leaching process. The pyrolysis vapour is separated into a condensable fraction (oil) and a non-condensable fraction (gas) thanks to a cross-flow condenser with air as indirect cooling medium. The remaining gas is compressed to 6 bar: a part of it is continuously converted in electricity for process use, while another part is stored for power generation at peak demand time. A flowsheet of the process is established and environmental and assessment of investments and production are discussed. For the pyrolytic treatment of 3 ton/hr of ELTs, the required heat for the reactor is 271 kW at 380 °C, provided by electrical heating elements. A reactor volume is determined for a residence time of about 6 h. For the cross-flow condenser, indirectly air-cooled, a heat-transfer area of about 13.2 m^2 is required. The compression of the gas the pressurized pyrolytic gas storage tank depends upon the excess pyrolytic gas produced during operation. The char cooler requires a heat-transfer area of 10.2 m^2, when indirectly cooled by water. Operating parameters of the leaching and subsequent recovery of Zn^{2+} complete the design. The product added-value and the large-scale capacity make the process economically viable, although the ROI is between 2 and 3 years.

1. Introduction

1.1. What are ELTs?

Once a tire has been used and cannot be retreaded – i.e. cannot be restored with new rubber and directly reused -, it becomes an end-of-life tire (ELT). Because of the many components present in tires, their recycling is quite difficult, all the more so as tire compositions can vary according to the producer specifications or the use (cars, trucks, buses, planes, etc.) Many authors have indexed different tire compositions, which are listed in Table 1 (Williams, 2013; Czajczynska et al., 2017; Antoniou and Zabaniotou, 2015; Martínez et al., 2013a; Papin et al., 2015; Debek and Walendziewski, 2015; Debek, 2019). Other components include textile and fabrics (nylon, kevlar) (~5 wt%), zinc oxide (0–2 wt%), sulphur (0–1 wt%), additives (0–3% wt), inert fillers such as silicates and alumina (≪ 1 wt%), accelerators and anti-ozonants (0–1 wt %) (Czajczynska et al., 2017; Antoniou and Zabaniotou, 2015; Martínez et al., 2013a). Contrary to ZnO that is used as vulcanisation catalyst and hence needs to be controlled in the char to guarantee a re-useable quality, the minor percentage of inert components will concentrate in the char, but will not affect its quality and reuse for new tire application.

A tire has furthermore different layers of different compositions for a better adhesion to the roads, and the presence of these different components does not facilitate the recycling. A scheme of a tire cross-section is represented in Fig. 1 (Czajczynska et al., 2017).

With about 17 million end-of-life tires each year (Zhang et al., 2020; Karagoz et al., 2020), recycling solutions need to be developed. Indeed, with the 1999/31/EC Directive (Martínez et al., 2013b), disposing of ELTs in landfills is very restricted: in 2020, only 4% of them are landfilled [(Williams, 2013)- (Martínez et al., 2013b)- (de Oliveira Neto et al., 2019)], where it can cause ground water pollution due to heavy metals (Malekzadeh, 2018; Gonçalves dos Santos et al., 2020), can provoke uncontrolled and hazardous fires [(Czajczynska et al., 2017)-(Gonçalves dos Santos et al., 2020)- (Pantea et al., 2003)], or a habitat for mosquitos and vermin [(Czajczynska et al., 2017)] [(Pantea et al., 2003)]. Furthermore, it takes 100 years for micro-organisms to degrade spent tires [(Czajczynska et al., 2017) (Papin et al., 2015) (Karagoz et al., 2020)]. For the remaining 96%, they are partly used as a fuel in ceramic and cement kilns (Pantea et al., 2003), but their pyrolysis with feedstock recovery is a growing perspective.

Indeed, pyrolysis allows to recover 71% of the energetic capacity of the tires, against only 42% for the simple combustion (Bouvier et al., 1987).

Pyrolysis processes have hence been initially biomass-driven and developed between 1960 and 1980 (Antoniou and Zabaniotou, 2015),

* Corresponding author.
E-mail address: renaud.ansart@toulouse-inp.fr (R. Ansart).

Symbols and abbreviations

A	Pre-exponential factor s^{-1}
A_{cond}, A_{cool}	Contact area of the condenser or the screw auger with char, respectively m^2
a_m	Specific particle surface area for heat transfer in the reactor $m^2.kg^{-1}$
CB	Carbon Black
c_i	Fraction of char in flow i
C_{pg}	Molar specific heat capacity of the gas $kJ.mol^{-1}.K^{-1}$
$c_{pm,i}$, $c_{pm,j}$	Specific heat capacity of flow i or component j, respectively $kJ.kg^{-1}.K^{-1}$
d_i	Inside diameter of the tubes m
d_p	Diameter of particles entering the reactor m
d_{screw}	Diameter of the screw cooler m
e	Wall thickness of the tubes mm
Ea	Apparent activation energy $kJ.mol^{-1}$
h, HTC	Local and overall convection heat transfer coefficient, respectively $W.m^{-2}.K^{-1}$
h_w	Apparent convection heat transfer coefficient of the tube wall $W.m^{-2}.K^{-1}$
I.D., O.D.	Inside and outside diameter of the tubes, respectively m
k, k_0	Overall kinetic rate constants s^{-1}
$k_{1\to6}$	Specific kinetic rate constants s^{-1}
k_C, k_f	Thermal conductivity of the char or fluid, respectively $W.m^{-1}.K^{-1}$
k_T	Kinetic and diffusion coupled constant s-1
L_0, L_1	Mass flow rates of input char with Zn^{2+} or output of Zn^{2+}-free char, respectively $kg.s^{-1}$
L_{cond}, L_{cool}	Length of the condenser tubes or screw cooler, respectively m
M	Inverse lever-arm point
$\dot{m}_i$	Mass rate of flow i $kg.s^{-1}$
$M_{Ca(OH)2}$, M_{Zn}	Molar weight of $Ca(OH)_2$ or Zn, respectively $g.mol^{-1}$
$\dot{n}$	Molar flow rate of the gas $mol.s^{-1}$
NR, SR	Natural or Synthetic Rubber, respectively
Nu	Nusselt number
P_i	Pressure of flow i Pa
Q	Power consumption kW
R	Ideal gas constant (R = 8.314) $J.mol^{-1}.K^{-1}$
S_0, S_1	Feedstock of solvent or outlet of solvent, respectively $kg.s^{-1}$
s_i, s_M	Fraction of solvent in flow i or in M, respectively
t	Time s
T ($\overline{T}$, T_i)	Temperature (average, of the flow i, respectively) K
TPO	Tire Pyrolysis Oil, as condensable pyrolysis fraction
U	Overall heat transfer coefficient $W.m^{-2}.K^{-1}$
V_i	Volume of flow i m^3
$\dot{v}_{ij}$	Volumetric flow rate of flow i in the section j $m^3.s^{-1}$
Vreactor	Volume of the reactor m^3
W	Work of the compressor kW
x_i	Fraction of component i
X_c	Conversion rate %
z_i	Fraction of Zn^{2+} in flow i
α	Dimensionless constant depending on γ
ΔH_p, ΔH_r, ΔH_{vap}	Enthalpy of the pyrolysis, reaction or evaporation, respectively $kJ.kg^{-1}$
ΔT_{lm}	Log-mean temperature K
γ	Dimensionless constant depending on C_{pg}
λ_j	Thermal conductivity of compound j $W.m^{-1}.K^{-1}$
μ_j	Dynamic viscosity of compound j Pa.s
ρ_j	Density of compound j $kg.m^{-3}$
τ	Residence time s

pyrolysis being the thermal degradation of the feedstock under an oxygen-free atmosphere (Williams and Brindle, 2002): in the presence of even minor percentages of oxygen, partial combustion will occur and this can lead to the formation of toxic furans, dioxins or benzopyrenes (Kaltaev et al., 2020). Furthermore, pyrolysis is an eco-friendly process (Betancur et al., 2020). Many pyrolysis technologies have been developed, and are classified into several categories according to the technique used to supply the endothermic heat of pyrolysis: conventional ones (combustion of non-condensable gas), or non-conventional ones (electrical heating, microwaves, ultrasounds, plasma, supercritical water and CO_2) (Januszewicz et al., 1359).

Prior to pyrolysis, metals and textiles/fabrics need to be separated and this is performed by sieving and magnetic separation after a multi-stage shredding (Papin et al., 2015; Debek and Walendziewski, 2015; Debek, 2019). Only crushed tire scraps remain as feedstock for pyrolysis. The main advantage of tire pyrolysis is that every product can be valorised and used as a new and alternative feedstock.

Firstly, the ELTs' char is very resistant to physical, chemical and biological degradation (Betancur et al., 2020) and can be directly recycled into the rubber industry (Budzyn and Tora, 2015), provided the composition of the enriched inert components in the char can be controlled. ZnO, present in the highest concentration, should preferably be removed since it will interfere during the vulcanisation of new rubber. Other inert (minerals) are also enriched in the char, but still at very low concentrations, which is admissible. Despite the minor contamination with filler materials, the char can also be transformed into high added value products, such as activated carbon [(Antoniou and Zabaniotou, 2015)][(Betancur et al., 2020)], feedstock for bitumen or printer's ink (Betancur et al., 2020), nanomaterials (Rambau et al., 2018) or even carbon black (Wu et al., 1997), which needs to accord to the ISO 1867–75.6 standard (Malekzadeh, 2018)][(Mikulova et al., 2013)].

Secondly, tire pyrolytic gas has a high calorific value and can be used to either supply the endothermic heat of the process itself or used for

Table 1
Composition of end-of-life tires.

Ref.	*Tire type*	NR - natural rubber (%)	SR - synthetic rubber (%)	*CB - carbon black (%)*	*metal (%)*	*others (%)*
Williams (2013)	*Car*	47		*21.5*	*16.5*	*15*
	Truck	45		*22*	*21.5*	*11.5*
Czajczynska et al. (2017)	*Car*	22	23	*28*	*13*	*14*
	Truck	30	15	*20*	*25*	*10*
Antoniou and Zabaniotou (2015)	*Car*	62.1		*31*	-	*6.9*
	Truck	45		*22*	*25*	*8*
Martínez et al. (2013a)	*Car*	14	27	*28*	*14*	*16–17*
	Truck	27	14	*28*	*14*	*16–17*
Papin et al. (2015)	*n.r.*	65		*25*	*10*	-
Debek and Walendziewski (2015))- (Debek (2019))	*n.r.*	60–65		*25–35*	-	*0–5*

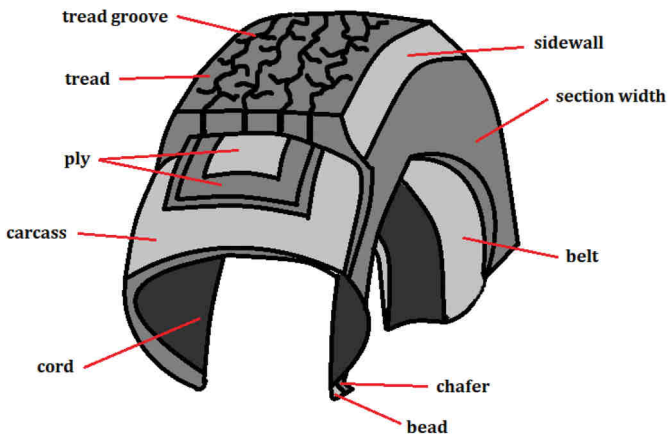

Fig. 1. Cross-section of a tire (adapted from (Czajczynska et al., 2017), copyright transfer granted by Elsevier).

power generation [(Williams and Brindle, 2002)][(Betancur et al., 2020)]. Its composition can vary, but it is mostly a mixture of CO_2, H_2, CO, N_2, C_xH_y. Its calorific value is about 37 MJ kg^{-1} (Martínez et al., 2013c). Pyrolytic gas can also be used for the formation of Zeolite Templated Carbons (Musyoka et al., 2018).

Finally, the tire pyrolysis oil (TPO) is considered an added-value product of the pyrolysis (Debek, 2019) and presents lots of economic advantages (Williams and Brindle, 2002), due to its high calorific value (44 MJ kg^{-1}) when desulfurized [(Karagoz et al., 2020)- (Hossain et al., 2020)] and its possibly fuel-blend with diesel [(Martínez et al., 2013b) (Karagöz et al., 2020)]. Furthermore, it can be used to strengthen polymer modified bitumen [(de Oliveira Neto et al., 2019) (Sharypov et al., 2016)], to make carbon-based nanomaterials (Rambau et al., 2018) or even to produce limonene (Januszewicz et al., 1359).

Test conditions however significantly affect product ratios and composition as illustrated in numerous publications (Williams, 2013)[(Kordoghli et al., 2016)- (Al-Salem, 2020)]. Since the composition of the incoming ELTs varies, the composition or the ratios of the products vary, hampering the separation of some co-products [(Antoniou and Zabaniotou, 2015) (Budzyn and Tora, 2015)]. However, some authors consider char and TPO as a limited source of revenue, unless new techniques are applied (Williams and Brindle, 2002) to e.g. remove sulphur from vulcanized tires or from their pyrolysis oil [(Czajczynska et al., 2017) (Zhang et al., 2020) (Karagöz et al., 2020)], or by upgrading the pyrolysis char.

1.2. *Objectives of the research*

The main objectives of the research are to examine and develop the design of an ELT pyrolysis plant with a leaching unit of $Zn^{2+}$from the char in order to improve its quality and to increase its sales' price and re-applicability. Leaching at a moderate pH will moreover not degrade the char itself, and Zn^{2+} can be recovered from the leachate by precipitation. The flowsheet of the unit to meet these objectives is represented in Fig. 2, including the mass flow rates and the temperatures. Firstly, a tire shredder, sieves and magnetic separator allow to remove metal and textile/fabrics from scrap tires, while reducing the particle size of the scrap rubber to below 2 or 3 mm. These particles will be fed to the pyrolysis reactor, built as a moving bed with electrical heating, thus avoiding a dilution of the pyrolysis products by the combustion gas if the endothermic heat was to be supplied by an internal partial combustion. A moving bed moreover allows to control the temperature profile along its height, and has a reduced pressure drop. The gas/vapour fraction is

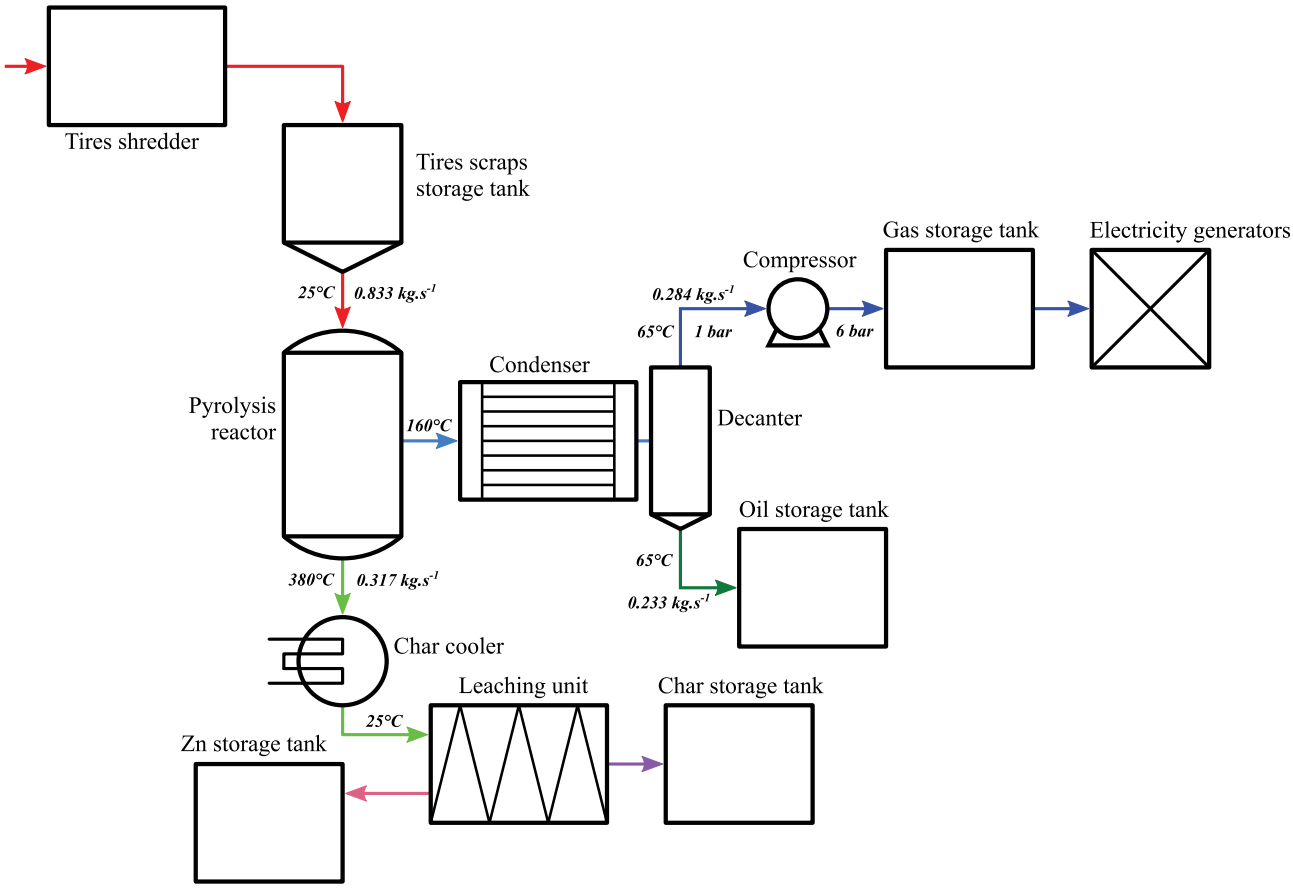

Fig. 2. Simplified flowsheet of the ELT pyrolysis process.

exhausted, vapours are condensed, and te residual non-condensable pyrolytic gas is compressed and stored for ultimate use in an electricity generator. The pyrolytic solid fraction, i.e. pyrolytic char, is cooled in a conveyor-cooler, and finally treated by leaching to remove the Zn^{2+} impurity.

Mass flow rates are given in Fig. 2.

With this flowsheet, the design can easily be divided into different parts, with clear and simple objectives. Firstly, all operation and reaction parameters of the pyrolysis reactor have to be gathered to enable its design. Secondly, the mixed vapour/gas condenser needs to be designed for a given coolant. Thirdly, the leaching unit needs to be sized, and finally the storage tanks need to be added. The pyrolytic gas needs to be stored for part of the time: it is indeed more profitable to buy electricity when its price is low (day and night time), and to use the gas to produce electricity when its price is higher (peak time). This variation of electricity prices is the result of the demand pattern (often referred to as the duck curve) which peaks in the morning (06–09 a.m.) and at night (06–11 p.m.). In Europe, peak electricity is rated over 3 times the price of the "valley" rating, e.g. 0.25 €/kWh in peak periods against 0.07 to 0.08 €/kWh for lean periods.

From the flow sheet of Fig. 2, the gas production rate is calculated at 0.2841 kg s^{-1}. With an energy content of 37 MJ/kg, the thermal combustion power accounts for 10.5 MW_{th}. If used in a gas-fired generator, about 3.1 MW_{el} can be generated, and the remaining 7.4 MW_{th} (cooling water + exhaust losses) can be used in a CHP concept. Since the pyrolysis plant will consume ~0.5 MW_{el}, there is ample scope for selling electricity to the grid, both in daytime, and at peak-time provided the pyrolytic gas is stored.

Some recommendations about the possible oil upgrading through desulfurization, or transformation of char into carbon black or activated carbon will also be included in the final recommendations.

2. Fundamentals of ELTs pyrolysis

2.1. Thermo-chemical and physical properties

The thermo-chemical and physical properties of all the flows of the process can be found in Supplementary Information, with the references used.

2.2. Kinetics

The first step to size a process is to determine the kinetics of the main reaction i.e. the pyrolysis of tire wastes. According to Al-Salem et al. (2009), the reaction can be represented by the following scheme:Fig. 3.

The liquid and/or aromatics produced are TPO or TPF, which can be revalorised and used as a fuel. The char is the solid fraction of the products, and the gas is a mix of non-condensable hydrocarbons. Al-Salem et al. (2009) developed the kinetic equations and determined the reaction rate constants, k_i.

Applying the Al-Salem et al. approach, the production of each product and reactant can be calculated. To do so, *Matlab 2019* ® was used with initialisation values of x_{ELTs} (t = 0) = 1, and x_A (t = 0) = x_L (t = 0) = x_G (t = 0) = x_C (t = 0) = 0.

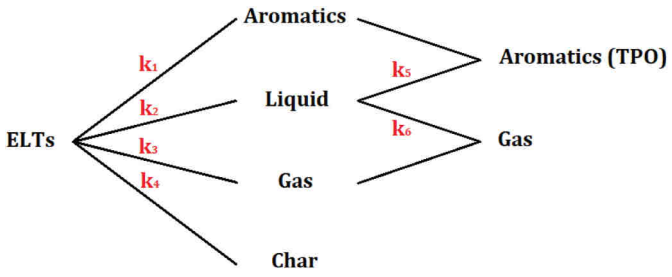

Fig. 3. Mechanism scheme of tire waste pyrolysis [adapted from 30].

Fig. 4 illustrates the model results at 500 °C, where no secondary reactions are observed. If the char production needs to be increased, the pyrolysis needs to be operated at a lower T, e.g. ~380 °C. The mechanism can be simplified by transforming it in a one-step parallel reaction, since no side reactions occur. The simplified mechanism is represented in Fig. 5, and described by equations (1)–(4).

$$\frac{dx_{ELTs}}{dt} = -x_{ELTs}.(k_1 + k_2 + k_3) \tag{1}$$

$$\frac{dx_O}{dt} = k_1.x_{ELTs} \tag{2}$$

$$\frac{dx_G}{dt} = k_2.x_{ELTs} \tag{3}$$

$$\frac{dx_C}{dt} = k_3.x_{ELTs} \tag{4}$$

To determine the values of the apparent activation energy and of the Arrhenius fitting pre-exponential factor, an overall kinetic rate constant at the proposed operation temperature is needed. According to (Bouvier et al., 1987), the overall kinetic rate constant at 372 °C is equal to k = 1.4*10^{-3} s^{-1}. This temperature should be ideal because this is the one at which the production of char is optimal.

The apparent activation energy and Arrhenius pre-exponential factor can be calculated (from Arrhenius law), from both Al-Salem et al. (2009) and Bouvier et al. (1987) results:

$$E_a = \frac{R.T_1.T_2.\ln\left(\frac{k_2}{k_1}\right)}{T_2 - T_1} = 56.5\ kJ.mol^{-1} \tag{5}$$

$$A = \frac{k_i}{\exp\left(-\frac{E_a}{R.T_i}\right)} = 52.53\ s^{-1} \tag{6}$$

Since the residence time is very long and kinetics very slow, the steady state approximation can be done, with equilibrium and constant compositions of the products achieved. It means that finally no specific kinetic rate constants of the different parallel and series reactions are needed to model the overall kinetics.

2.3. Heat and mass balances

To determine the power consumption of the reactor, calculations must include the enthalpy of the reaction, the specific heat capacities (The Engineering Toolbox., 2020; Gas Encyclopedia by Air L, 2020; ChemSpider. Search and sh, 2020), and the mass rates of the products. With these values given in Fig. 2 and in Supplementary Information, equation (7) determines the reactor power consumption:

$$Q_{input} = \dot{m}_{tire}.\delta H_r = \dot{m}_{tire}.\delta H_p + \sum_i c_{pm,i}.\dot{m}_i.\left(T_{outlet,i} - T_{inlet,tire}\right) \tag{7}$$

With *i* representing char, gas and oil properties. The enthalpy of reaction is given in Supplementary Information, ΔH_r = 325 kJ kg^{-1}. The outlet temperature of the oil and gas, in the form of a vapour, is not the same as the outlet temperature of the char, since the vapour and gas exchange their sensible heat with the incoming cold feedstock in the preheating section of the reactor. Since the ELT particles are preheated in the reactor, the gas and vapour outlet temperature is 160 °C.

A power consumption of Q_{inlet} = 271 kW is hence calculated. The reactor should hence be equipped with 150 heating elements of 2 kW each.

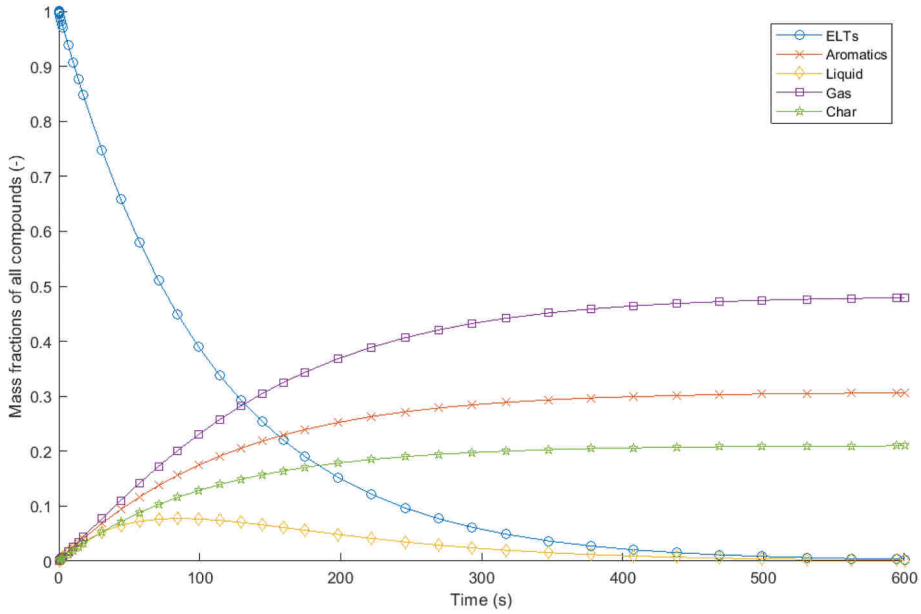

Fig. 4. Fractions of compounds with time.

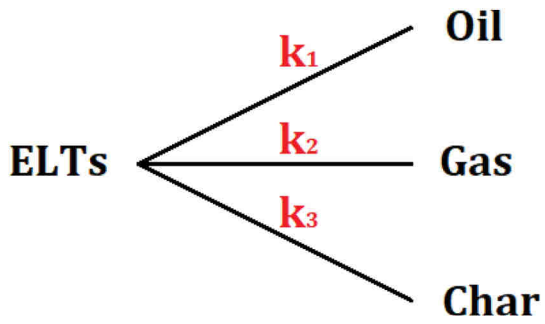

Fig. 5. Simplified mechanism scheme of tire waste pyrolysis.

3. Essential plant components

3.1. Pyrolysis reactor

To size the reactor, the residence time required for the pyrolysis reaction is needed, which is affected by the diffusion in the char. According to Kunii & Levenspiel (Kunii and Levenspiel, 1969), the required residence time τ for a conversion rate X_C can be described when diffusion and reaction kinetics are competing with the following equation:

$$1 - X_C = \exp(-k_T.\tau) \tag{8}$$

Where

$$\frac{1}{k_T} = \frac{1}{k} + \frac{1}{k_C} \tag{9}$$

With k the overall kinetic rate constant, and k_C the diffusion resistance, expressed by the following equation (Kunii and Levenspiel, 1969):

$$k_C = \frac{Nu.k_f.a_m}{d_p.c_{pm}} \tag{10}$$

Since no detailed data for ELT heat transfer are available, but since ELTs are of similar nature to poly methyl methacrylate (PMMA), known values of PMMA were used (Smolders and Baeyens, 2004), however obtained in a fluidized bed pyrolysis. At average properties of the ELT and products (see Table 2 or Supplementary Information), the Nusselt number can be calculated. In a fixed bed, operated at lower superficial gas velocities, heat transfer is lower than in a fluidized bed (Kunii and Levenspiel, 1969), Considering the pyrolytic vapour and gas flows, the superficial velocity will be about 0.3 m s^{-1}. To fluidized the same particles in a well-mixed condition, velocities in excess of 1.5 m s^{-1} will be required. The Reynolds number will hence be a at least a fivefold in a fluidized bed application. For the fixed bed application, with Re ~5, Nu will be 0.025. In the fluidized bed application, Re will be 25 with Nu ~7.5. A reduction from fluidized to fixed bed by a factor of 300 is hence deemed necessary, as shown in Table 2 (Kunii and Levenspiel, 1969).

Table 2
Physico-chemical properties used for calculations.

k_f (W.m^{-1}.K^{-1})	0.15
d_p *(mm)*	*1*
a_m (m^2.kg^{-1})	*10*
$Nu_{fluidised}$ (−) (Smolders and Baeyens, 2004)	$6.4*10^{-3}$
Nu_{fixed} (−) (Kunii and Levenspiel, 1969)	$2.14*10^{-3}$

Although the higher superficial velocity will considerably reduce the size of a fluidized bed reactor (I.D), a moving packed bed reactor is favoured for its ease of residence time control and its temperature gradient along the bed height, hence slowly heating the fed tire particles to pyrolysis temperature.

The diffusion coefficient can be calculated with equation (10) as k_C = $1.605*10^{-5}$ s^{-1}. Since the kinetic rate constant k is much higher than k_C, the heat diffusion is the major reaction resistance.

The residence time is fixed from equation (8), equal to τ = 22,222 s (or ~ 6 h), which leads to a volume of $V_{reactor}$ = 30.86 m^3.

3.2. Tire pyrolysis oil condensation

After the feedstock preheating section of the pyrolysis reactor, gases and vapours are exhausted at 160 °C. The production rates are estimated at 0.233 kg s^{-1} of condensable vapours (with boiling point in excess of 110 °C), and 0.284 kg s^{-1} of non-condensable gases (CO, H_2, CO_2, C_nH_{n+2} with n < 6). The condenser can hence be considered in a three-step approach: *(i)* the cooling from 160 to 110 °C; *(ii)* the condensation of organics at 110 °C; and *(iii)* the deep-cooling of the non-condensable gases to 65 °C.

An air-cooled condenser is proposed. A water-cooled condenser

could possibly be used, but would require a secondary water-air cooler since cooling water can only be discharged in the river at a temperature exceeding the feed temperature by 6 °C. A cross-flow exchanger is suggested, since the available ambient air is unlimited. Physico-chemical properties of the different streams are given in Supplementary Information. Given that the tubes have a thermal conductivity of $\lambda_{tube} = 15$ W m^{-1}. K^{-1}, and with a tube wall thickness $e \leq 2$ mm, the conductive resistance to heat transfer can be neglected since corresponding to $h_w > 7500$ W m^{-2}. K^{-1}, in comparison with $h \ll 100$ W m^{-2}. K^{-1} for vapour, gas and air flows.

Considering the mass flow rates of the different exhaust components, the heat balance is fixed for all three sections, given that the vaporisation enthalpy is equal to $\Delta H_{vap} = 300$ kJ kg^{-1}:

(i) 160–110 °C: 24.5 kW
(ii) Condensation at 110 °C: 69.8 kW
(iii) 110–65 °C: 22.7 kW

Since air will be used as cooling medium, its feed temperature is assumed to be ambient, i.e. an average 20 °C. A scheme representing the temperatures and flows variations is depicted in Fig. 6. Since condensed pyrolytic oil was removed in section 2, section 3 only deals with non-condensables.

At the prevailing average temperatures, flows can be expressed in m^3. h^{-1} or m^3. s^{-1} using the respective densities at the prevailing operation temperatures in the different sections of the condenser. The calculated values can be found in Fig. 6.

Similarly, the logarithmic mean temperatures are defined for the cross-flow operation:

$$\delta T_{lm,i} = \frac{\left(T_{inlet,i,1} - T_{outlet,i,2}\right) - \left(T_{outlet,i,1} - T_{inlet,i,2}\right)}{\ln\left(\frac{T_{inlet,i,1} - T_{outlet,i,2}}{T_{outlet,i,1} - T_{inlet,i,2}}\right)} \quad (11)$$

With i the section number, 1 the gas/vapour flow and 2 the air flow. The results are:

(i) $\Delta T_{lm} = 106.5$ °C
(ii) $\Delta T_{lm} = 82.3$ °C
(iii) $\Delta T_{lm} = 58.7$ °C

Since the operation is of cross-flow nature, a correction factor should be applied (VDI-Wärmeatlas and Ca5, 1974), calculated at 0.7 to 0.8. This will however be included in a design safety margin of 30%.

Knowing the volumetric flow rates, the operating temperatures and the gas/air/vapour properties, heat transfer coefficients were determined from VDI-Wärmeatlas, differently for gas/vapour inside the tubes (VDI-Wärmeatlassection, 1974a) and for cross-flow of air (VDI-Wärmeatlassection, 1974b). The velocities were all taken at 10 m s^{-1} for the air flow and 12 m s^{-1} for the gas/vapour flow (in view of the higher average temperature). All the calculations steps have been made for each section of the condenser, and result in heat transfer coefficients of $HTC = 116$ W m^{-2}. K^{-1} for air, $HTC = 52$ W m^{-2}. K^{-1} for section 1, $HTC = 43$ W m^{-2}. K^{-1} for section 2 and $HTC = 44.7$ W m^{-2}. K^{-1} for section 3 respectively.

The flow rate of the vapour/gas determines the required flow cross section of the tubes. If standard tubes of 20 mm I.D. (24 mm O.D.) are selected, the required cross-sectional area at 12 m s^{-1} for the lowest average temperature of 87.5 °C is:

$$\frac{0.408\ m^3/s}{12\ m/s} = 0.076\ m^2 \quad (12)$$

With tubes of 20 mm I.D., 242 parallel tubes are required.

It should be noted that at higher temperatures, the same number and geometry of pipes will increase the velocity, which enhances the heat transfer coefficient, and hence serves as a design safety margin. The final design is illustrated in Fig. 7, assuming a safety design factor of 15%. Pipes will be arranged on a triangular pitch, with pitch size of 10 mm (to provide the required air velocity of 10 m s^{-1}). 9 rows will need to be stacked.

The size of the heat exchanger can be further reduced if the heat transfer tubes are fitted with outer fins, since the air-tube wall heat transfer coefficient will be enhanced by a factor of 1.4–1.5 in comparison with the bare tube due to the extra surface area exposed and with considering the fin efficiency, although the cost of the finned tubes needs to be outweighed against the limited gain in size (the lower heat transfer coefficient inside the tube however remains a major heat transfer resistance).

3.3. Gas compression and storage

After the gas is separated from the oil in the condenser, it needs to be stored in a gas tank at 6 bar. The flow rate of the gas leaving the condenser is 0.284 kg s^{-1}, which represents about 1112 m^3 h^{-1} at 1 bar.

The power required from 1 bar to 6 bar can be calculated with the

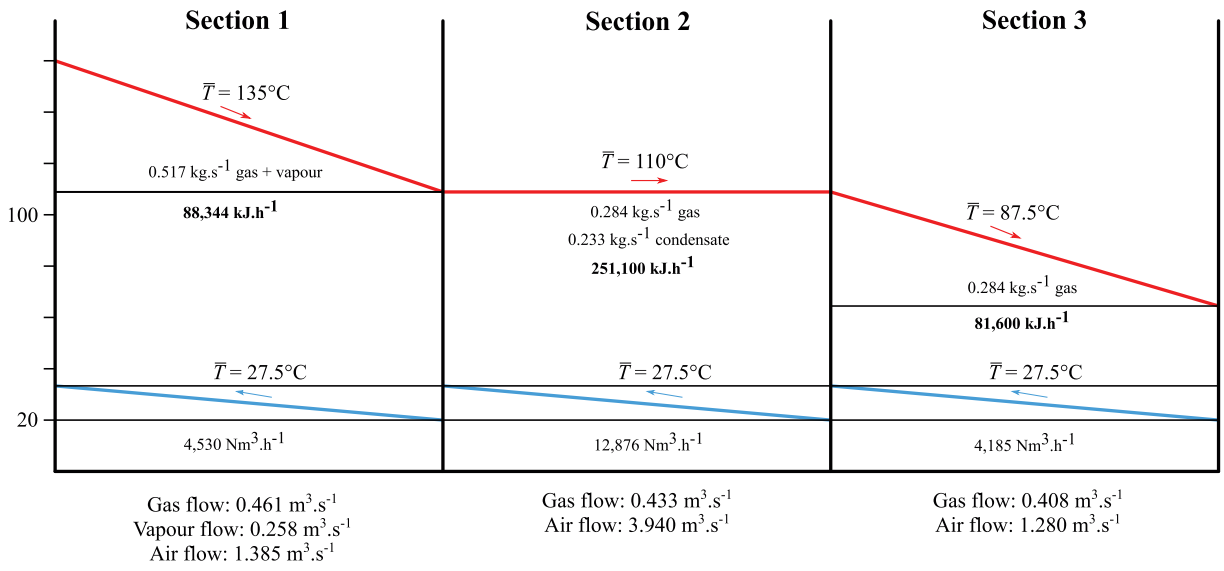

Fig. 6. Heat and mass balances in the condenser.

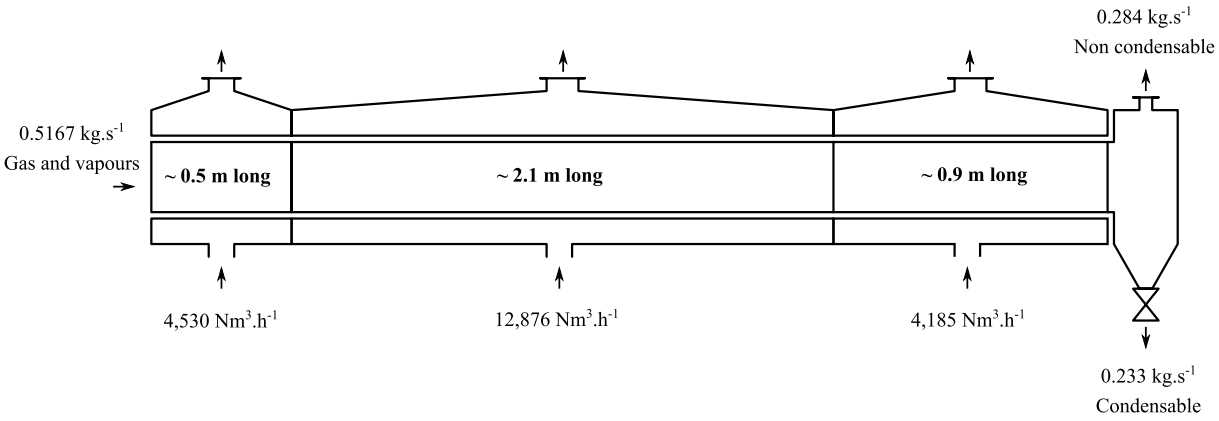

Fig. 7. Design of the condenser.

procedure used by Kang et al. (2018), with $\dot{n}$ being the molar flow rate of 12.33 mol s^{-1}, T_1 the inlet temperature of 65 °C, P_1 and P_2 respectively the inlet and outlet pressure of 1 and 6 bar, and α and γ two dimensionless constants defined by the specific heat capacities of the gas at constant volume and pressure. Since mixed gases are present, only assumptions can be made on its composition. An average value of 1.2 kJ kg^{-1}. K^{-1} is taken. The constants are defined with C_{pg} being the molar specific heat capacity, equal to 0.02766 kJ mol^{-1}. K^{-1}. Then, with $\gamma = 1.4298$ and $\alpha = 2.3267$, a work of $W = 57.53$ kW is required for the given pyrolytic gas flow rate and the pressure increase of 1 bar–6 bar. With the Laplace law the storage volume needed can now be calculated. To enable a production at peak times (8 h/day), 8900 m^3 of pyrolytic gas needs to be stored. A storage at 6 bar is hence insufficient to reduce the size of the storage tank. It is proposed to store the gas at 25 bar in a storage tank of 360 m^3. The compressor power will hence increase ($W =$ 131.54 kW) but the stored volume allows operation during the complete peak time.

3.4. Oil storage

With a flow rate of 838.8 kg h^{-1}, it represents 1.323 m^3 h^{-1}. If the installation is assumed to work 10 h a day and that the oil is sold once daily, a storage tank of 13.23 m^3 is needed, i.e. 15–20 m^3 including a security margin.

As said in Introduction, pyrolytic oil is currently sold as a precursor of a new renewable fuel. It can also be used for the bulk of interesting chemical compounds which can be found in it: for example, limonene, toluene, styrene [(Williams, 2013) (Januszewicz et al., 1359)], as further discussed in the recommendations.

3.5. Char cooling

The outlet temperature of the char from the pyrolysis reactor being 380 °C, it needs to be cooled to ambient temperature (25 °C) before being treated and sold. A screw cooler with both concentric water-cooled scroll housing and water-cooled shaft and flights (Engineering Talk and ash scr, 2010) is used.

The water used in the cooler is taken from a river at a temperature of 20 °C, which will return to it after the cooling process. The cooling medium could be air, but since it would an indirect one, heat transfer coefficient would be dominated by air-wall coefficient, which would lead to a twice bigger screw cooler. Another solution could be to cool the char from 380 °C to 100 °C with water, and then to end the cooling with air. The injection of water droplets on the hot char might however lead to a thermal decrepitation, resulting in unwanted particle attrition.

To avoid thermal pollution of the river, a maximal temperature of 26 °C is allowed. For that reason, the water is air cooled with a VXI-18.0 air cooler from Baltimore Aircool ©, which can cool 4.7 L per seconds (aircoil company, 2020). Since the water use needs to be limited, a satisfying flow rate of 1.5 l s^{-1} is fixed.

The heat needed for the cooling of $Q = 90.14$ kW, and the outlet temperature of the water of 34.65 °C are determined.

As for the sizing of the condenser, the exchange area required is fixed, if the assumption of $U = 110$ W m^{-2}. K^{-1} is made (Dewil et al., 2007), a heat transfer coefficient predicted for particles of a similar size in a mixed heat transfer system. A slightly higher value is obtained by applying the heat transfer theory developed by Baeyens and Geldart (1980) for particles of similar dimensions and with a residence time of0.2–0.4 s at the cooling wall. The required indirect cooling area is $A =$ 10.20 m^2.

For a screw cooler with a diameter of $d_{screw} = 0.6$ m, since it will be half full, the exchange area can be expressed with the following equation.

$$A = \frac{1}{2} * 2.\pi.L.\frac{d_{screw}}{2} \quad (13)$$

The required length will then be 10.82 m, or 11 m with a safety margin.

If indirect air cooling was applied, the required length would be about 22 m, hence executed as a cascade of 2 screw conveying coolers in series, since screw conveyor lengths are limited to about 12 m for mechanical support of the scroll shaft.

3.6. Leaching unit

To be able to sell the char at added-value, Zn^{2+} needs to be removed. Indeed, before being used for tires, the rubber is vulcanized to increase its resistance, but the zinc needs to be removed for the tire process if the char is to be used as filler. A continuous perforated belt extractor as illustrated in numerous handbooks, e.g. Perry's Chemical Engineering or (Keith Roper et al., 2011) is the most efficient technology for this use, even if it is expensive, but it can be a good economic investment. Leaching is a process used to extract a solute from a solid thanks to a solvent (Wikipedia. Leaching (chem, 2020).

In the leaching, a solvent is needed, which will be chosen based on two criteria: the char will not be soluble in it, but Zn^{2+} ions will. Furthermore, the solvent needs to have a low pH: indeed, as can be seen on the solubility curves of zinc dependent on the pH (Fig. 8). At a pH of 4, nearly all Zn^{2+} will be soluble (Liu and Gao, 2015). HCl with a concentration of 10^{-4} $mol.L^{-1}$ can be used. Nevertheless, it is impossible to remove all the zinc from the char because of mass transfer limitations and limited solubility at a given pH, but most of it can be removed with a residence time of 30 min according to experimental results.

To size the leaching unit, some assumptions are made. Firstly, the solvent feed flow rate S_0 will be the same as the char feed one L_0, i.e. 0.317 kg s^{-1} or 1140 kg h^{-1}. Secondly, there will be no solvent in the

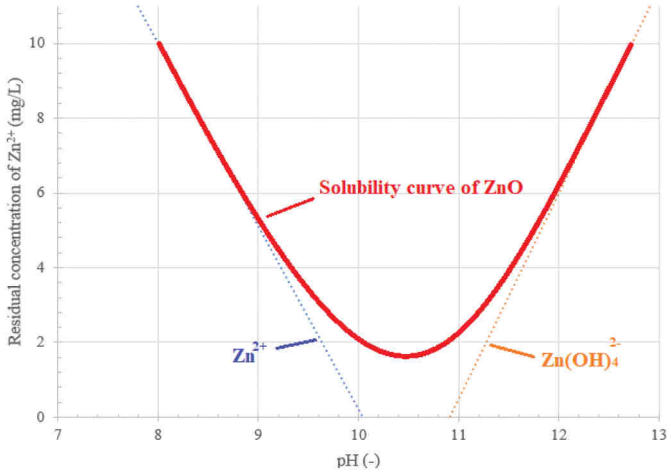

Fig. 8. Solubility curves of zinc with pH [adapted from 44].

char feed (the char will be completely dry), and no char in the solvent outlet flow S_1. Thirdly, an assumption which will be verified later, that there is no zinc in the solvent feed. The fraction of zinc in the char feed is $z_{L0} = 0.05$ (Liu and Gao, 2015) and the fraction of char in the char outlet flow is $c_{L1} = 0.7$ which means that the voids of the flow are filled with the solvent.

To determine the missing values, a z-s diagram is used, depicted in Fig. 9. According to the definition of a fraction, the following equation needs to be verified at every moment:

$$c_i + z_i + s_i = 1 \tag{14}$$

Where i is the considered flow, c stands for the char fraction, z for the zinc fraction and s for the solvent one.

For the underflow L_1, since c_{L1} is known, the statement that $1 - c_{L1} = 0.3$ is made which allows us to draw the underflow line (- - - -), since it crosses the z-axis at 0.3 and has a slope of −1. The overflow line will be parallel to the latter, and crosses the s-axis at 1, since the assumption that $s_{S0} = 1$ has been made (….). With the zinc fraction of the char feed $z_{L0} = 0.05$, the full line can be drawn (___), in which an M point can be put, used in the inverse lever arm rule. Its coordinate on s-axis can be found thanks to equation (15).

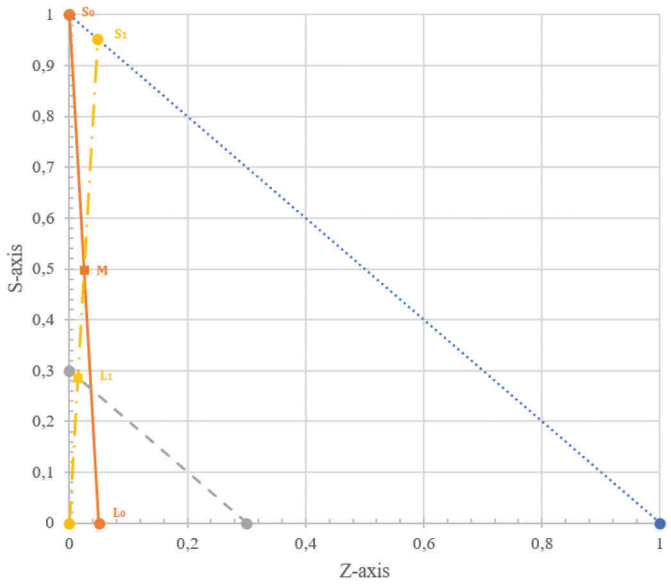

Fig. 9. z-s diagram of the leaching unit.

$$\frac{L_0}{S_0} = \frac{s_{S0} - s_M}{s_M - s_{L0}} = 1 \tag{15}$$

Thanks to that point, the underflow point L_1 is defined and the overflow point S_1 as the intersection of the line which passes from the origin to the M point (. _. _.) and with respectively the underflow line and the overflow line, which will give us the fractions of the outlets.

Then, the flow rates of L_1 and S_1 need to be known. Since only char will be in the underflow, and with the assumption that there is no mass loss, all the char present in L_0 will be in L_1. With this hypothesis, L_1 can be determined thanks to the following equation:

$$c_{L0}.L_0 = c_{L1}.L_1 \tag{16}$$

If the inverse lever arm rule is repeated with L_1 and S_1, the overflow rate is determined, since all the fractions are known. All the values and their signification have been listed in Table 3.

With densities of the char and HCl of Supplementary Information, the volumetric flow rates of $L_0 = 1.77\ m^3\ h^{-1}$ and $S_0 = 1.43\ m^3\ h^{-1}$ are determined, and since the residence time is 30 min, it means that a minimum of 1.6 m^3 is required for the belt extractor.

To be able to recycle the solvent and to recover zinc for a future utilisation, the pH needs to be increased at 9, as shown in Fig. 8. For that, $Ca(OH)_2$ is used, with which zinc will be able to form insoluble $Zn(OH)_2$, which can be sold at a good price. The amount of $Ca(OH)_2$ needed is determined by the following chemical equation:

$$Zn^{2+} + 2(OH)^- \rightarrow Zn(OH)_2 \tag{17}$$

Thus, to convert the most of Zn^{2+} as possible, twice the amounts as $Ca(OH)_2$ is needed. With the molar weight of Zn and $Ca(OH)_2$, according to the values in Table 4, 79.22 kg h^{-1} of $Ca(OH)_2$ is required. Since $CaCl_2$ will be formed when adding HCl to the $Ca(OH)_2$ recycled solvent, $CaCl_2$ will progressively increase in concentration. Although the solubility of $CaCl_2$ is very high in both acid and alkaline environments, the recycled solvent will need to be purged at intermittent times (and fed to the wastewater treatment) to eliminate the increasing $CaCl_2$ concentrations.

To be able to re-use the solvent in the process, the pH needs to be decreased back to 4. For that, some fresh HCl with a lower pH is added to complete the flow which will be used as solvent feed. Since the flow rate leaving the diluter unit is of 733 kg h^{-1}, 307 kg h^{-1} is added to complete the solvent feed. Thanks to the conservation of molar rates, the pH of the fresh solvent needed to have a final pH of 4 can now be determined, with the following equation:

$$pH_{final} = -\log\left(\frac{1,140*10^{-4} - 733*10^{-9}}{307}\right) = 3.43 \tag{18}$$

According to Fig. 8, the residual concentration of Zn will be 0.1 mg. L^{-1} in the flow at pH 4. Since it will be diluted with fresh HCl, there would be 91.62 mg h^{-1} Zinc in the flow, which represent a fraction of

Table 3
Properties of the flows in the leaching unit.

Char feed flow rate	L_0 (kg.h^{-1})	1140
Fraction of char in L_0	*c_{L0} (−)*	*0.95*
Fraction of zinc in L_0	*z_{L0} (−)*	*0.05*
Fraction of solvent in L_0	*s_{L0} (−)*	*0*
Solvent feed flow rate	*S_0 (kg.h^{-1})*	*1140*
Fraction of char in S_0	*c_{S0} (−)*	*0*
Fraction of zinc in S_0	*z_{S0} (−)*	*0*
Fraction of solvent in S_0	*s_{S0} (−)*	*1*
Solvent overflow rate	*S_1 (kg.h^{-1})*	*733*
Fraction of char in S_1	*c_{S1} (−)*	*0*
Fraction of zinc in S_1	*z_{S1} (−)*	*0.0477*
Fraction of solvent in S_1	*s_{S1} (−)*	*0.9523*
Char underflow rate	*L_1 (kg.h^{-1})*	*1547*
Fraction of char in L_1	*c_{L1} (−)*	*0.7*
Fraction of zinc in L_1	*z_{L1} (−)*	*0.0143*
Fraction of solvent in L_1	*s_{L1} (−)*	*0.2857*

Table 4
Summary of Investment and Production for a 3 T/h plant (12,000 T/year).

Investments items	€
Crushing, screening, conveying (3 T/h)	*1,200,000*
Feeding, Reactor (300 kW)	*1,500,000*
Electricity generators (1 × 500 kW (process use), 2 × 1.5 MW for grid integration)	*1,090,000*
Pyrolytic oil storage	*80,000*
Pyrolytic gas compression and storage	*600,000*
Char cooling and storage (container)	*170,000*
ZnO leaching	*100,000*
Erection, instrumentation, electrical connections (20% of above)	*948,000*
Total	*5,688,000*
Production	
Pyrolytic oil (T/year)	*3312*
Pyrolytic gas (T/year) - equivalent to 3.1 MW_{el}	
-Process use - about 0.5 MW_{el}	
-Annual power sold to the grid	
** Daytime 0.9 MW_{el} (4000 h/year)*	
** Peaktime 3 MW_{el} (2000 h/year)*	
Pyrolytic char (T/year)	*4565*

zinc calculated as follows:

$$z_{S0} = \frac{92.10^{-6}\ kg/h}{1,140\ kg/h} = 8.07{*}10^{-8} \quad (19)$$

It is indeed negligible, which validates our assumptions.

3.7. Possible upgrading

With the previous char upgrading, it will be sold at a better price, but the oil and the gas will not. To be able to increase the profit, some modifications can be undertaken, for the oil and the gas as well as for the Zn-free char.

Many authors encourage to desulfurize the oil, to increase its price, as well as to decrease risks: with the presence of sulphur, the TPO can be considered as hazardous: indeed, SO_2 is very toxic, and can lead to the formation of H_2SO_4, which provokes acid rain. To do so, many processes have been analysed. Firstly, desulphurisation in a CFB or a BFB have been studied (Deng et al., 2019). Secondly, some scientists consider the best way to do it is via a selective adsorption with Al_2O_3 coupled with an ODS (oxidative desulphurisation) with H_2O_2 (Zhang et al., 2020), while some other researchers consider the more efficient method to be the hydro-refining of the oil (at 3 MPa, 380 °C and with NiMo–Al_2O_3 as a catalyst) [(Debek and Walendziewski, 2015)- (Debek, 2019)]. Some authors propose a pre-treatment with H_2SO_4 and activated CaO, followed by an ODS under vacuum can be the solution [(Karagoz et al., 2020) (Karagöz et al., 2020)], purify TPO with a S–ZrO_2/SBA-15-H_2O_2 catalytic oxidation method (Hossain et al., 2020). The TPO as precursor can also be used for carbon nanomaterials, since traditional feedstock is limited (Rambau et al., 2018).

Table 5
Summary of Investment and Production for a 3 T/h plant (12,000 T/year).

Investments items	€
Crushing, screening, conveying (3 T/h)	*1,200,000*
Feeding, Reactor (300 kW)	*1,500,000*
Electricity generators (1 × 500 kW (process use), 2 × 1.5 MW for grid integration)	*1,090,000*
Pyrolytic oil storage	*80,000*
Pyrolytic gas compression and storage	*600,000*
Char cooling and storage (container)	*170,000*
ZnO leaching	*100,000*
Erection, instrumentation, electrical connections (20% of above)	*948,000*
Total	*5,688,000*
Production	
Pyrolytic oil (T/year)	*3312*
Pyrolytic gas (T/year) - equivalent to 3.1 MW_{el}	
-Process use - about 0.5 MW_{el}	
-Annual power sold to the grid	
** Daytime 0.9 MW_{el} (4000 h/year)*	
** Peaktime 3 MW_{el} (2000 h/year)*	
Pyrolytic char (T/year)	*4565*

In addition, char can also be upgraded into carbon black with a post pyrolysis treatment (Williams, 2013), while it has improved physical properties (Mikulova et al., 2013) and is a better adsorbent than char (Malekzadeh, 2018). However, it would require other operating conditions than analysed before to maximize its production (Betancur et al., 2020). The char can also be activated with steam or CO_2 (physical way) or with KOH, $ZnCl_2$ or H_3PO_4 (chemical way) (Antoniou and Zabaniotou, 2015), while it has many uses and is frequently sought-after (Williams, 2013).

Finally, the gas is currently used to produce heat and power, but could also be used to produce hydrogen with a post pyrolysis treatment at 800 °C, with Ni–Mg–Al catalyst and with oxygen (Williams, 2013). Furthermore, it can be used to make Zeolite Templated Carbons, used to store hydrogen or for batteries (Musyoka et al., 2018). As the gas is the tire pyrolysis product which has the lowest value, upgrading it could be an interesting way to increase the revenues generated by the plant.

4. Environmental and economic assessment

4.1. Environmental assessment

Since the industrial plant has the goal to recycle wastes into energy or new high value products, it is by nature eco-friendly. Since it does not use the TPG heat directly for the pyrolysis reactor, volatile hazardous compounds are not released, and e.g. an emission saving of 129,980 tonnes per year of CO_2 has been calculated.

Furthermore, all the pyrolysis products are valorised are re-used, no waste is generated during the process, which enables to meet environmental requirements.

4.2. Economic data

To know if the process designed in this project is economically viable, the equipment purchasing cost and the sales' revenue of the pyrolysis products could bring need to be determined. The investments and production are analysed in the following table, and the Return on Investment is also calculated below.

Operational costs are the sum of mainly salaries (2 engineers, 6 operators: 500,000 €/year), maintenance at 5% of the total investment (300,000 €/year), overheads and insurance at 300,000 €/year. Additional costs of chemicals (HCl, $Ca(OH)_2$) and water supply are negligible. Towards values of the products, conservative commercial applications were used, i.e. pyrolytic oil at 120 €/ton, upgraded pyrolytic char at 300 €/ton and daytime electricity at 0.075 €/kWh and 0.25 €/kWh at peak time. Total sales revenues are hence ~3.5 million €/year. The Return on Investment (ROI) is then calculated as the ratio of investment and revenue after accounting for the operating cost. In this case, with the average costs, the ROI is about 2.4 years. Without any upgrading, the process is then viable, since most of the societies would invest in a project for which the ROI is less than 3 years. Furthermore, the possible upgrading discussed in part 3.7. could decrease the ROI even more. Finally, value of pyrolysis products will increase as more stringent legislation of secondary fuels will be implemented.

5. Conclusion

This paper has investigated the recycling process of end-of-life tires via a pyrolysis reaction. Different parts of the process have been

analysed and calculations have been performed for a plant capacity of 3 tons per hour. The most essential plant components are the reactor, the condenser and the leaching unit. Firstly, for the reactor, the heat and mass balance revealed that 271 kW heat input is required in order to keep the reactor at a temperature of 380 °C. The power consumption of the reactor is delivered by electrical heating elements, and the dimensions of the reactor are approximately 10 m height and 2 m diameter. Secondly, the vapours are separated into a gas fraction and into an oil fraction in a three-sections cross-flow condenser with air as indirect cooling medium. The remaining gas is compressed to 25 bar and used to generate electricity, while the oil is sold to (petro-) chemical companies. The char is cooled in screw cooler and Zn^{2+} is removed from it in a leaching unit to increase sales' price.

Authors contribution

Niezgoda A, Investigation, Methodology, Original draft, Writing - review & editing, Visualization. Deng Y, Conceptualization, Data curation, Original draft, Writing - review & editing. Sabatier F, Validation, Writing - review & editing, Supervision. Ansart R, Methodology, Writing - review & editing, Project administration, Funding acquisition

Declaration of competing interest

The authors declare that they have no known competing financial interests or personal relationships that could have appeared to influence the work reported in this paper.

Appendix A. Supplementary data

Supplementary data to this article can be found online at https://doi.org/10.1016/j.jenvman.2020.111318.

References

aircoil company, Baltimore. Vxi 9. last consultation on 06/07/2020. *https://www.baltimoreaircoil.eu/en/products/VXI-9-36*, 36.

Al-Salem, S.M., 2020. Valorisation of end of life tyres (ELTs) in a newly developed pyrolysis fixed bed batch process. Process Saf. Environ. Protect. 138, 167–175.

Al-Salem, S.M., Letteieri, P., Baeyens, J., 2009. Kinetics and product distribution of end of life tyres (ELTs) pyrolysis: a novel approach in polyisoprene and SBR thermal cracking. J. Hazard Mater. 172, 1690–1694.

Antoniou, N., Zabaniotou, A., 2015. Experimental proof of concept for a sustainable end of life tyres pyrolysis with energy and porous materials production. J. Clean. Prod. 101, 323–336.

Baeyens, J., Geldart, D., 1980. Modelling approach to the effect of equipment scale on fluidized bed heat transfer data. J. Powder Bulk Solids Technology 4, 1–10.

Betancur, M., Arenas, C.N., Martínez, J.D., Navarro, M.V., Murillo, R., 2020. CO_2 gasification of char derived from waste tire pyrolysis: kinetic models comparison. Fuel, 273 117745.

Bouvier, J.M., Charbel, F., Gelus, M., 1987. Gas-solid pyrolysis of tire wastes – kinetics and material balances of batch pyrolysis of used tires. Resour. Conserv. 15, 205–214.

Budzyn, S., Tora, B., 2015. Analysis of Carbon Black from Tyres Pyrolysis. Journal of the Polish Mineral Engineering Society. Inzynieria Mineralna – LIPIEC – GRUDZIEN - July – December.

ChemSpider. Search and share chemistry. last consulting on 02/07/2020. *https://www.chemspider.com/*.

Czajczynska, D., Kryzynska, R., Jouhara, H., Spencer, N., 2017. Use of pyrolytic gas from waste tire as a fuel: a review. Energy 134, 1121–1131.

de Oliveira Neto, G.C., Carvalho Chaves, L.E., Rodrigues Pinto, L.F., Curvelo Santana, J. C., Castro Amorim, M.P., Ferreira Rodrigues, M.J., 2019. Economic, environmental and social benefits of adoption of pyrolysis process of tires: a feasible and eco-friendly mode to reduce the impacts of scrap tires in Brazil. Sustainability 11, 2076.

C. Debek. Modification of pyrolytic oil from waste tyres as a promising method for light fuel production. Materials 12 880, 2019.

Debek, C., Walendziewski, J., 2015. Hydro refining of oil from pyrolysis of whole tyres for passenger cars and vans. Fuel 159, 659–665.

Deng, Y., Ansart, R., Baeyens, J., Zhang, H., 2019. Flue gas desulphurization in circulating fluidized beds. Energies 12 3908.

Dewil, R., Appels, L., Baeyens, J., 2007. Improving the heat transfer properties of waste activated sludge by advanced oxidation processes. Mater. Sci. 1.

Engineering Talk, ash screw cooler. last consultation on 06/07/2020. *http://engineering-power-plant.blogspot.com/2010/07/ash-screw-cooler.html*.

Gas Encyclopedia by Air Liquide. last consulting on 02/07/2020. *https://encyclopedia.airliquide.com/*.

Gonçalves dos Santos, R., Lucas Rocha, C., Lopes Souza Felipe, F., Tonon Cezario, F., Correia, P.J., Rezaei-Gomari, S., 2020. Tire waste management: an overview from chemical compounding to the pyrolysis-derived fuels. J. Mater. Cycles Waste Manag. 22, 628–641.

Hossain, M.N., Choi, M.K., Park, H.C., Choi, H.S., 2020. Purifying of waste tire pyrolysis oil using an S-ZrO_2/SBA-15-H_2O_2 catalytic oxidation method. Catalysts 10, *368*.

K. Januszewicz, P. Kazimierski, W. Kosakowski, W. M. Lewandowski. Waste tyres pyrolysis for obtaining limonene. Materials 13 1359, 2020.

Kaltaev, A. Zh, Larionov, K.B., Yankovsky, S.A., Slyusarsky, K.V., Gubin, V.E., 2020. Production of black carbon by steam pyrolysis (thermolysis) method of rubber waste in the form of worn-out automobile tires. AIP Conference Proceedings 2212, 020023.

Kang, Q., Dewil, R., Degrève, J., Baeyens, J., Zhang, H., 2018. Energy analysis of a particle suspension solar combined cycle power plant. Energy Convers. Manag. 163, 292–303.

Karagoz, M., Uysal, C., Agbulut, U., Saridemir, S., 2020. Energy, exergy, economic and sustainability assessments of a compression ignition diesel engine fueled with tire pyrolytic oil – diesel blends. J. Clean. Prod. 264, 121724.

Karagöz, M., Agbulut, Ü., Saridemir, S., 2020. Waste to energy: production of waste tire pyrolysis oil and comprehensive analysis of its usability in diesel engines. Fuel 275, 117844.

Keith Roper, D., Seader, J.D., Henley, Ernest J., 2011. Separation Process Principles Chemical and Biochemical Operations. Wiley.

Kordoghli, S., Paraschiv, M., Khiari, B., Zagrouba, F., Tazerout, Mohand, 2016. Using oxides of alkaline-earth metals as catalysts in used tyres pyrolysis. International Journal of Chem Tech Research 9 (8), 359–365.

Kunii, D., Levenspiel, O., 1969. Fluidization Engineering (Chapter 7). John Wiley and Sons, Inc., New York, pp. 210–215.

Liu, Y., Gao, W., 2015. Growth process, crystal size and alignment of zno nanorods synthesized under neutral and acid conditions. J. Alloys Compd. 629, 84–91.

Malekzadeh, M., 2018. Comparison the capacity of base treated pyrolytic carbon toward Cu(II), Pb(II) and Cr(III) removal from water. International Proceedings of Chemical, Biological and Environmental Engineering 103, *4*.

Martínez, J.D., Puy, N., Murillo, R., García, T., Navarro, M.V., Mastral, A.M., 2013a. Waste tyre pyrolysis – a review. Renew. Sustain. Energy Rev. 23, 179–213.

Martínez, J.D., Lapuerta, M., García-Contreras, R., Murillo, R., García, T., 2013b. Fuel properties of tire pyrolysis liquid and its blends with diesel fuel. Energy Fuels 27, 3296–3305.

Martínez, J.D., Murillo, R., García, T., Veses, A., 2013c. Demonstration of the waste tire pyrolysis process on pilot scale in a continuous auger reactor. J. Hazard Mater. 261, 637–645.

Mikulova, Z., Sedenkova, I., Matejova, L., Vecer, M., Dombek, V., 2013. Study of carbon black obtained by pyrolysis of waste scrap tyres. J. Therm. Anal. Calorim. 111, 1475–1481.

Musyoka, N.M., Rambau, K.M., Manyala, N., Ren, J., Langmi, H.W., Mathe, M.K., 2018. Utilization of waste tyres pyrolysis vapour in the synthesis of Zeolite Templated Carbons (ZTCs) for hydrogen storage application. Journal of Environmental Science and Health, Part A 53. No. 11 1022-1028.

Pantea, D., Darmstadt, H., Kaliaguine, S., Roy, C., 2003. Heat-treatment of carbon blacks obtained by pyrolysis of used tires. Effect on the surface chemistry, porosity and electrical conductivity. J. Anal. Appl. Pyrol. 67, 55–76.

Papin, A.V., Ignatova, A. Yu, Makarevich, E.A., Nevedrov, A.V., 2015. Preparation of composite fuel-based carbon black pyrolysis of tires (Russian). UDC 504.064.

Rambau, K.M., Musyoka, N.M., Manyala, N., Ren, J., Langmi, H.W., Mathe, M.K., 2018. Preparation of carbon nanofibers/tubes using waste tyres pyrolysis oil and coal fly ash derived catalyst. Journal of Environmental Science and Health, Part A 53 (No. 12 1115), 1122>.

Sharypov, V.I., Kiselev, V.P., Beregotsova, N.G., Kemenev, N.V., Kuznetsov, B.N., 2016. Use of liquid products of nitrile rubber tires pyrolysis for synthesis of bitumen modifiers (Russian). *UDC 678.049*, *2*, *665–775*.

Smolders, K., Baeyens, J., 2004. Thermal degradation of PMMA in fluidised beds. Waste Manag. 24, 849–857.

The Engineering Toolbox. *https://www.engineeringtoolbox.com/*, last consulting on 13/07/2020.

VDI-Wärmeatlas, 1974. section Ca5.

VDI-Wärmeatlas, 1974a. section Gb.

VDI-Wärmeatlas, 1974b. section Gd.

Wikipedia. Leaching (chemistry). last consulting on 13/07/2020. https://en.wikipedia.org/wiki/Leaching_(chemistry.

Williams, P.T., 2013. Pyrolysis of waste tyres: a review. Waste Manag. 33, 1714–1728.

Williams, P.T., Brindle, A.J., 2002. Catalytic pyrolysis of tyres: influence of catalyst temperature. Fuel 81, 2425–2434.

Wu, S.-Y., Su, M.-F., Baeyens, J., 1997. The fluidized bed pyrolysis of shredded tyres: the influence of carbon particles, humidity, and temperature on the hydrodynamics. Powder Technol. 93, 283–290.

Zhang, Q., Zhu, M., Jones, I., Zhang, Z., Zhang, D., 2020. Desulfurization of spent tire pyrolysis oil and its distillate via combined catalytic oxidation using H_2O_2 with formic acid and selective adsorption over Al_2O_3. Energy Fuels 34, 6209–6219.